

# The Influence of Ionic Strength on Yttrium and Rare Earth Element Complexation by Fluoride Ions in $\text{NaClO}_4$ , $\text{NaNO}_3$ and $\text{NaCl}$ Solutions at 25 °C

Yu-Ran Luo · Robert H. Byrne

Received: 8 August 2006 / Accepted: 21 November 2006 /

Published online: 1 May 2007

© Springer Science+Business Media, LLC 2007

**Abstract** Stability constants of the form  ${}_F\beta_1(\text{M}) = [\text{MF}^{2+}][\text{M}^{3+}]^{-1}[\text{F}^-]^{-1}$  (where  $[\text{MF}^{2+}]$  represents the concentration of a yttrium or a rare earth element (YREE) complex,  $[\text{M}^{3+}]$  is the free YREE ion concentration, and  $[\text{F}^-]$  is the free fluoride ion concentration) were determined by direct potentiometry in  $\text{NaNO}_3$  and  $\text{NaCl}$  solutions. The patterns of  $\log_{10} {}_F\beta_1(\text{M})$  in  $\text{NaNO}_3$  and  $\text{NaCl}$  solutions very closely resemble stability constant patterns obtained previously in  $\text{NaClO}_4$ . For a given YREE, stability constants obtained in  $\text{NaClO}_4$  were similar to, but consistently larger than  ${}_F\beta_1(\text{M})$  values obtained in  $\text{NaNO}_3$  which, in turn, were larger than formation constants obtained in  $\text{NaCl}$ . Stability constants for formation of nitrate and chloride complexes ( ${}_{\text{NO}_3}\beta_1(\text{M}) = [\text{MNO}_3^{2+}][\text{M}^{3+}]^{-1}[\text{NO}_3^-]^{-1}$  and  ${}_{\text{Cl}}\beta_1(\text{M}) = [\text{MCl}^{2+}][\text{M}^{3+}]^{-1}[\text{Cl}^-]^{-1}$ ) derived from  ${}_F\beta_1(\text{M})$  data exhibited ionic strength dependencies generally similar to those of  ${}_F\beta_1(\text{M})$ . However, in contrast to the somewhat complex pattern obtained for  ${}_F\beta_1(\text{M})$  across the fifteen member YREE series, no patterns were observed for nitrate and chloride complexation constants: neither  ${}_{\text{NO}_3}\beta_1(\text{M})$  nor  ${}_{\text{Cl}}\beta_1(\text{M})$  showed discernable variations across the suite of YREEs. Nitrate and chloride formation constants at 25 °C and zero ionic strength were estimated as  $\log_{10} {}_{\text{NO}_3}\beta_1^0(\text{M}) = 0.65 \pm 0.06$  and  $\log_{10} {}_{\text{Cl}}\beta_1^0(\text{M}) = 0.71 \pm 0.05$ . Although these constants are identical within experimental uncertainty, the distinct ionic strength dependencies of  ${}_{\text{NO}_3}\beta_1(\text{M})$  and  ${}_{\text{Cl}}\beta_1(\text{M})$  produced larger differences in the two stability constants with increasing ionic strength whereby  ${}_{\text{Cl}}\beta_1(\text{M})$  was uniformly larger than  ${}_{\text{NO}_3}\beta_1(\text{M})$ .

**Keywords** Rare earth elements · Fluoride complexation · Nitrate complexation · Chloride complexation · Stability constants · Ionic strength · Lanthanide · Yttrium

## 1 Introduction

Yttrium and rare earth (YREE) abundances in the environment are strongly influenced by both solution complexation and sorption [1]. Differences in the affinities of solution ligands

Y.-R. Luo · R.H. Byrne (✉)

College of Marine Science, University of South Florida, St. Petersburg, Florida 33701, USA

e-mail: byrne@marine.usf.edu

for YREEs across the fifteen member series, as well as variations in the affinities of sorptive surfaces for different YREEs, cause the relative environmental solution concentrations of YREEs to differ considerably from their relative abundances in the minerals from which they are derived. Observations of changes in relative YREE concentrations (i.e., YREE fractionation) has become an important means of assessing the fundamental nature of YREE exchange between solutions and solids in the natural environment [2].

Comparative YREE concentrations (abundance ‘patterns’) can be determined with high precision. As such, in order to meaningfully evaluate the nature of environmental YREE sorption from observations of (1) YREE environmental abundance patterns and (2) aqueous complexation behavior (e.g., Byrne and Kim [3], Lee and Byrne [4], and Quinn et al. [2]), the precision of YREE stability constant patterns must be quite high. In order to produce precise accounts of the relative magnitudes of YREE stability constants it is, in general, essential that stability constants are determined as a full 15-member suite using consistent procedures. Compilations of YREE stability constants obtained several at a time in different laboratories, or even several at a time by different investigators in the same laboratory, are unlikely to exhibit highly coherent patterns. The patterns of  $\text{MF}^{2+}$  formation constants shown in Fig. 1 were initially obtained potentiometrically [5] and were reproduced in the cation exchange investigation of Luo and Millero [6] following the procedures of Schijf and Byrne [7]. The general shape of the pattern shown in Fig. 1 is also in good accord with results obtained [8] using solvent exchange radiochemical REE analyses for five REEs (Ce, Eu, Gd, Tb and Yb) plus linear free energy relationships to estimate other YREE stability constants. All of the observations that led to the summary of constants shown in Fig. 1 were obtained in either  $\text{NaClO}_4$  [5] or dilute ( $\sim 0.025 \text{ mol}\cdot\text{kg}^{-1}$ )  $\text{NaNO}_3$  [6, 7].

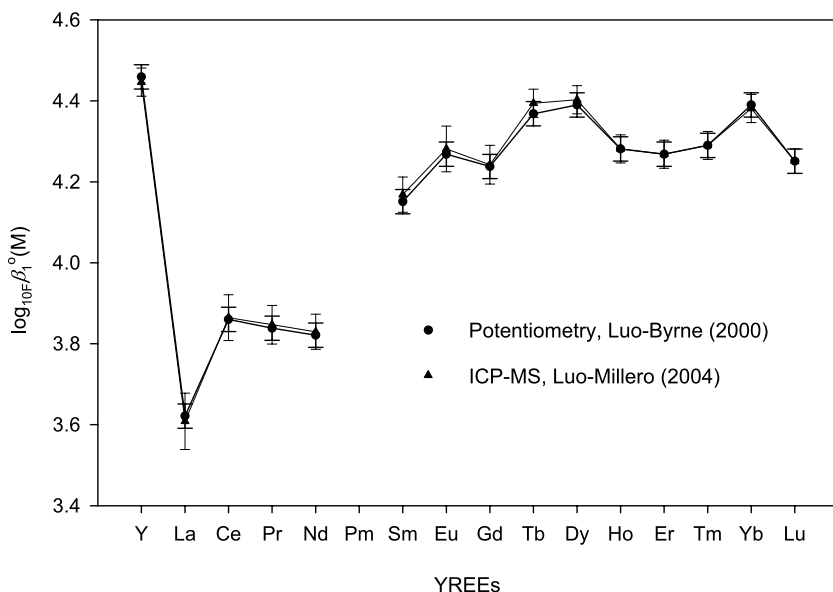


**Fig. 1** Comparisons between  $\log_{10} \beta_1^0 (M)$  determined in  $\text{NaClO}_4$  [5] and  $\text{NaNO}_3$  [6]. As is the case for a wide variety of YREE complexes,  $\text{MF}^{2+}$ , stability constants do not exhibit a smooth monotonic increase between La and Lu. The stability constant pattern for YREE fluoride complexes is, for example, quite similar to the patterns obtained for methylmalonic acid, dimethylmalonic acid and DL-2-hydroxy-2,3-dimethylbutanoic acid [4]

Only a small number of additional investigations (Walker and Choppin [9], Avramenko et al. [10], Bilal and coworkers [11–14], Becker and Bilal [15], Menon and coworkers [16, 17]) have provided assessments of fluoride stability constants across the entire suite of REEs. Among these investigations, the results of Menon and coworkers [16, 17], and Bilal and coworkers [11–14] obtained in NaNO<sub>3</sub> and NaCl, respectively, reproduce the general aspects of the pattern in Fig. 1 (large changes between La and Eu, and relatively small changes between Tb and Lu) but do not exhibit sufficient precision to make more detailed comparisons meaningful (see Fig. 1 of Lee and Byrne [8]). The results of Walker and Choppin [9] and Avramenko et al. [10], characterized by smoothly increasing equilibrium constants between La and Gd, and between Gd and Lu, are in poor accord with both the general formation constant trends reported by Bilal and coworkers [11–15], Menon et al. [16, 17], and Lee and Byrne [8], as well as the detailed patterns shown in Fig. 1. Apparently the experiments of Walker and Choppin [9] and Avramenko et al. [10] were subject to unknown experimental problems.

Due to the relatively poor precision of the results obtained by Bilal and coworkers [11–15] and Menon et al. [16, 17], there are currently no precise, comprehensive assessments of YREE fluoride stability constants in NaNO<sub>3</sub> medium, and no precise determinations of YREE fluoride stability constants in NaCl medium other than those of Luo and Byrne [18] at 0.7 mol·kg<sup>-1</sup> and 3 mol·kg<sup>-1</sup> ionic strength. In the present work, we have extended the investigations of Luo and Byrne [5, 18] to include YREE fluoride stability constant determinations in NaCl and NaNO<sub>3</sub> over a range of ionic strengths between 0.7 and 5.0 mol·kg<sup>-1</sup>. Comparison of results obtained in NaCl and NaNO<sub>3</sub> with previous results obtained in NaClO<sub>4</sub> allows determination of YREE chloride and YREE nitrate stability constants over a wide range of ionic strength. Observations of  $c_1\beta_1$  as a function of ionic strength are essential for improved assessments of rare earth element speciation in seawater.

## 2 Theory

The potentiometric procedures used in this work closely follow those described by Luo and Byrne [5, 18]. YREE stability constants in the form

$${}_F\beta_1(M) = \frac{[MF^{2+}]}{[M^{3+}][F^-]} \quad (1)$$

where brackets denote molal concentrations {moles·(kg-H<sub>2</sub>O)<sup>-1</sup>} of YREE fluoride complexes, MF<sup>2+</sup>, free YREE ions, M<sup>3+</sup>, and fluoride ions, F<sup>-</sup>, were determined at 25 °C over a wide range of ionic strength. Fluoride ion concentrations were measured with a fluoride specific ion electrode calibrated in terms of free F<sup>-</sup> concentrations at constant ionic strength (*I*). Our electrode calibrations demonstrated that electrode potentials (*E*) versus fluoride concentration, expressed as log<sub>10</sub>[F<sup>-</sup>], were Nernstian (*S* = -59.16 mV at 25 °C). Calibration constants (*E*<sup>o</sup>) in Eq. 2,

$$E = E^o + S \log_{10}[F^-], \quad (2)$$

were determined at each ionic strength in each experimental medium (NaClO<sub>4</sub>, NaNO<sub>3</sub>, and NaCl). Total fluoride concentrations ([F<sup>-</sup>]<sub>T</sub>) in our experiments were on the order of 1 × 10<sup>-4</sup> mol·kg<sup>-1</sup>, and total YREE concentrations ([M<sup>3+</sup>]<sub>T</sub>) were greater than or equal to 1 × 10<sup>-3</sup> mol·kg<sup>-1</sup>. The concentration of the MF<sup>2+</sup> complex was calculated from the following equation

$$[MF^{2+}] = [F^-]_T - [F^-] - [HF^0] \quad (3)$$

where  $[\text{HF}^0]$  is the concentration of hydrofluoric acid. The concentration of  $[\text{HF}^0]$  in each experiment was calculated from experimental measurements of  $[\text{F}^-]$  and  $[\text{H}^+]$ , and  $\text{HF}^0$  formation constants ( $K_{\text{HF}} = [\text{HF}^0][\text{H}^+]^{-1}[\text{F}^-]^{-1}$ ) taken from NIST [19]. Because the pH in our solutions was approximately two units larger than the  $\log_{10} K_{\text{HF}}$  values in each experimental solution,  $[\text{HF}^0]$  concentrations were quite small relative to free fluoride ion concentrations.

Free YREE concentrations were calculated from the relationship

$$[\text{M}^{3+}] = [\text{M}^{3+}]_{\text{T}} - [\text{MF}^{2+}]. \quad (4)$$

Determinations of  $[\text{F}^-]$ ,  $[\text{MF}^{2+}]$  and  $[\text{M}^{3+}]$  using Eq. 2 through 4 then allow calculation of  ${}_{\text{F}}\beta_1(\text{M})$  via Eq. 1.

Stability constants for formation of  $\text{MNO}_3^{2+}$  and  $\text{MCl}^{2+}$  were calculated following the procedures of Luo and Byrne [18]:

$${}_{\text{NO}_3}\beta_1(\text{M}) = \frac{[\text{MNO}_3^{2+}]}{[\text{M}^{3+}][\text{NO}_3^-]} = \left( \frac{{}_{\text{F}}\beta_1(\text{M})_{\text{NaClO}_4}}{{}_{\text{F}}\beta_1(\text{M})_{\text{NaNO}_3}} - 1 \right) [\text{NO}_3^-]^{-1} \quad (5)$$

$${}_{\text{Cl}}\beta_1(\text{M}) = \frac{[\text{MCl}^{2+}]}{[\text{M}^{3+}][\text{Cl}^-]} = \left( \frac{{}_{\text{F}}\beta_1(\text{M})_{\text{NaClO}_4}}{{}_{\text{F}}\beta_1(\text{M})_{\text{NaCl}}} - 1 \right) [\text{Cl}^-]^{-1}. \quad (6)$$

### 3 Materials and Methods

The experimental methods used in this work are very similar to those employed in the previous investigations of Luo and Byrne [5, 18]. YREEs were obtained from Aldrich Chemical with a purity of 99.9% or better. All salts were oxides except for those of Ce(III) and Tb(III), which were obtained as nitrates. Sodium perchlorate (anhydrous, minimum 99%), sodium chloride (minimum 99.5%) and sodium nitrate (ACS,  $\geq 99.0\%$ ) were obtained from Sigma. Sodium hydroxide (purified) and perchloric acid (70% ultrapure reagent) were obtained from J.T. Baker. High-purity  $\text{N}_2$  was obtained from South Air Products (UHP/ZERO grade) and was scrubbed of  $\text{CO}_2$  with an OMI indicating purifier (SUPELCO, Bellefonte, PA).

YREE stock solutions were prepared by dissolving the salts in  $5 \text{ mol}\cdot\text{L}^{-1}$  aqueous  $\text{HClO}_4$ . The compositions of stock solutions ( $0.1 \text{ mol}\cdot\text{kg}^{-1}$  YREEs) were verified with an Agilent 4500 ICP-MS calibrated with standards obtained from SPEX (Metuchen NJ).  $\text{NaClO}_4$ ,  $\text{NaNO}_3$  and  $\text{NaCl}$  solutions were filtered through  $0.45\text{-}\mu\text{m}$  polycarbonate membranes. Experimental solutions ( $\text{NaClO}_4$ ,  $\text{NaNO}_3$  and  $\text{NaCl}$ ) were placed in a polyethylene beaker within a thermostatted ( $25.0 \pm 0.1 \text{ }^\circ\text{C}$ ) glass beaker. Solutions were stirred gently and continuously scrubbed with  $\text{CO}_2$ -free  $\text{N}_2$ .

Fluoride ion concentrations and pH were monitored concurrently with a Corning model 130 pH meter and an Orion 720A meter, respectively. Solution pH measurements involved the use of a Ross-type combination pH electrode (Orion No. 800500) and fluoride ion concentration measurements were made with a fluoride-ion selective combination electrode (Accumet 13-620-528). The pH electrode was calibrated on the free hydrogen ion concentration scale via volumetric additions of perchloric acid to unbuffered  $\text{NaClO}_4$ ,  $\text{NaNO}_3$ , and  $\text{NaCl}$  solutions. The fluoride electrode was calibrated (at high pH) in each experimental medium through volumetric additions of  $0.01 \text{ mol}\cdot\text{L}^{-1}$  sodium fluoride. Electrode responses were Nernstian within  $\pm 0.5\%$  ( $\pm 0.3 \text{ mV}$ ).

#### 4 Results and Discussion

Stability constants for the formation of YREE fluoride complexes ( $\text{MF}^{2+}$ ) over a wide range of ionic strength are shown in Table 1 ( $\text{NaClO}_4$  medium) and Table 2 ( $\text{NaNO}_3$  and  $\text{NaCl}$ ). The data shown in Table 1 were fit as a function of ionic strength using Eq. 7

$$\log_{10}\text{F}\beta_1(\text{M}) = \log_{10}\text{F}\beta_1^0(\text{M}) - \frac{3.066I^{0.5}}{1 + BI^{0.5}} + CI. \quad (7)$$

The data in Table 2 were also fit using Eq. 7. But, in the absence of data at ionic strengths below  $0.7 \text{ mol}\cdot\text{kg}^{-1}$ , fits of data obtained in  $\text{NaNO}_3$  and  $\text{NaCl}$  were constrained to have intercepts ( $\log_{10}\text{F}\beta_1^0(\text{M})$ ) identical to those obtained in fits of the  $\text{NaClO}_4$  data. The parameters obtained in Eq. 7 fits of Tables 1 and 2 data are shown in Table 3, and typical fit results, using Gd as an example, are shown in Fig. 2. Quality of fit depictions are shown as residual plots ( $\Delta \log_{10}\text{F}\beta_1(\text{M}) = (\log_{10}\text{F}\beta_1(\text{observed}) - \log_{10}\text{F}\beta_1(\text{predicted}))$ ) in Fig. 3a ( $\text{NaClO}_4$ ), Fig. 3b ( $\text{NaNO}_3$ ) and Fig. 3c ( $\text{NaCl}$ ). The residuals shown in Fig. 3a indicate that the quality of the data fits is not significantly dependent on the YREE identity. Observations and predictions agree within approximately 0.06 log units for all YREEs, and no distinct patterns in the residuals are observed across the suite of YREEs. The largest residuals in Fig. 3a were obtained at  $0.015$  and  $0.1 \text{ mol}\cdot\text{kg}^{-1}$  ionic strength. For ionic strengths between  $0.4$  and  $6.0 \text{ mol}\cdot\text{kg}^{-1}$ ,  $\log_{10}\text{F}\beta_1(\text{M})$  predictions and observations generally agree within 0.04 log units. The depiction of residuals shown in Fig. 3b is bimodal. For the heavy rare earths, predictions and observations obtained in  $\text{NaNO}_3$ , generally agree within 0.04 log units. For the light rare earths, residuals as large as 0.06 are observed. Figure 3c shows that Eq. 7 and the data shown in Table 3 provide a very good summary of the  $\log_{10}\text{F}\beta_1(\text{M})$  data. Residuals are generally smaller than 0.03.

Alternative descriptions of the Table 1 and 2 formation constant data can be obtained using Eq. 7 in the form generally used for SIT analysis:

$$\log_{10}\text{F}\beta_1(\text{M}) = \log_{10}\text{F}\beta_1^0(\text{M}) - \frac{3.066I^{0.5}}{1 + 1.5I^{0.5}} + CI. \quad (8)$$

Table 4 shows best fit results obtained using Eq. 8 ( $B = 1.5$ ). Figures 4a, 4b and 4c show, as expected, that residuals obtained with only two fitted parameters ( $\log_{10}\text{F}\beta_1^0(\text{M})$  and  $C$ ) are somewhat larger than those obtained for three fitted parameters ( $\log_{10}\text{F}\beta_1^0(\text{M})$ ,  $B$  and  $C$ ). Comparisons of Figs. 3 and 4 show that residuals, using either Eq. 7 or Eq. 8, are smallest for  $\text{NaCl}$ . In addition, the comparative quality of fits for  $\text{NaCl}$  (Fig. 3c versus Fig. 4c) are in better accord than is the case for Eq. 7 versus Eq. 8 fits of the data obtained in perchlorate and nitrate solutions. Inspection of Table 3 shows the basis of this result. The ‘ $B$ ’ parameters obtained for  $\text{NaCl}$  (Table 3) range between 1.38 and 1.48 for the light rare earths and between 1.53 and 1.60 for the heavy rare earths. Since these values are on average near 1.5, two parameter (Eq. 8) and three parameter (Eq. 7) fits will not be considerably different. In contrast, the ‘ $B$ ’ parameters obtained for  $\text{NaNO}_3$  are as low as 1.27 and, in  $\text{NaClO}_4$ , as large as 1.82. In these cases it is expected that two-parameter and three-parameter fits will differ significantly.

Tables 3 and 4 provide estimates of  $\log_{10}\text{F}\beta_1^0(\text{M})$  obtained in  $\text{NaClO}_4$ ,  $\text{NaNO}_3$  and  $\text{NaCl}$ . The  $\log_{10}\text{F}\beta_1^0(\text{M})$  uncertainties in Table 3, which are based on data obtained in  $\text{NaClO}_4$ , are on the order of  $\pm 0.035$ , significantly smaller than the uncertainties appropriate to  $\text{NaClO}_4$  ( $\pm 0.05$ ) shown in Table 4. The  $\log_{10}\text{F}\beta_1^0(\text{M})$  uncertainties obtained in  $\text{NaNO}_3$  (Table 4) are on the order of 0.05 for the light YREEs and 0.025 for the heavy YREEs. The  $\log_{10}\text{F}\beta_1^0(\text{M})$

**Table 1**  $\log_{10} F\beta_1(M)$  data ( $\text{NaClO}_4$ ) at 25 °C {molal ( $\text{mol}\cdot\text{kg}^{-1}$ ) scale}. These data, originally obtained by Luo and Byrne [5] are reported here because the original  $\log_{10} F\beta_1(M)$  data of Luo and Byrne [5] were erroneously reported in molar ( $\text{mol}\cdot\text{L}^{-1}$ ) units

	$I$ ( $\text{mol}\cdot\text{kg}^{-1}$ )										
	0.015	0.1	0.4	0.7	1.5	3.0	4.0	5.0	6.0		
Y	4.18 ± 0.03	3.79 ± 0.03	3.59 ± 0.03	3.52 ± 0.03	3.52 ± 0.03	3.60 ± 0.03	3.72 ± 0.03	3.81 ± 0.04			
La	3.38 ± 0.03	2.95 ± 0.03	2.74 ± 0.03	2.68 ± 0.03	2.69 ± 0.03	2.77 ± 0.03	2.88 ± 0.03	3.16 ± 0.04			
Ce	3.61 ± 0.03	3.20 ± 0.03	2.98 ± 0.03	2.89 ± 0.03	2.90 ± 0.03	3.01 ± 0.03	3.12 ± 0.03	3.36 ± 0.04			
Pr	3.59 ± 0.03	3.18 ± 0.03	2.95 ± 0.03	2.89 ± 0.03	2.89 ± 0.03	2.97 ± 0.03	3.10 ± 0.03	3.31 ± 0.04			
Nd	3.56 ± 0.03	3.15 ± 0.03	2.94 ± 0.03	2.88 ± 0.03	2.88 ± 0.03	2.95 ± 0.03	3.09 ± 0.03	3.30 ± 0.04			
Pm											
Sm	3.91 ± 0.03	3.49 ± 0.03	3.28 ± 0.03	3.21 ± 0.03	3.21 ± 0.03	3.25 ± 0.03	3.40 ± 0.03	3.48 ± 0.04			3.59 ± 0.04
Eu	4.04 ± 0.03	3.58 ± 0.03	3.40 ± 0.03	3.33 ± 0.03	3.33 ± 0.03	3.38 ± 0.03	3.52 ± 0.03	3.59 ± 0.04			3.71 ± 0.04
Gd	3.99 ± 0.03	3.55 ± 0.03	3.37 ± 0.03	3.29 ± 0.03	3.29 ± 0.03	3.35 ± 0.03	3.45 ± 0.03	3.56 ± 0.04			3.67 ± 0.04
Tb	4.12 ± 0.03	3.72 ± 0.03	3.51 ± 0.03	3.40 ± 0.03	3.42 ± 0.03	3.49 ± 0.03	3.63 ± 0.03	3.72 ± 0.04			3.80 ± 0.04
Dy	4.13 ± 0.03	3.73 ± 0.03	3.52 ± 0.03	3.44 ± 0.03	3.43 ± 0.03	3.50 ± 0.03	3.65 ± 0.03	3.73 ± 0.04			3.83 ± 0.04
Ho	4.01 ± 0.03	3.61 ± 0.03	3.41 ± 0.03	3.34 ± 0.03	3.34 ± 0.03	3.41 ± 0.03	3.54 ± 0.03	3.63 ± 0.04			3.73 ± 0.04
Er	4.00 ± 0.03	3.61 ± 0.03	3.41 ± 0.03	3.33 ± 0.03	3.33 ± 0.03	3.41 ± 0.03	3.53 ± 0.03	3.62 ± 0.04			3.74 ± 0.04
Tm	4.02 ± 0.03	3.63 ± 0.03	3.42 ± 0.03	3.34 ± 0.03	3.35 ± 0.03	3.43 ± 0.03	3.55 ± 0.03	3.63 ± 0.04			3.73 ± 0.04
Yb	4.11 ± 0.03	3.73 ± 0.03	3.52 ± 0.03	3.44 ± 0.03	3.45 ± 0.03	3.52 ± 0.03	3.65 ± 0.03	3.73 ± 0.04			3.86 ± 0.04
Lu	3.98 ± 0.03	3.59 ± 0.03	3.37 ± 0.03	3.29 ± 0.03	3.30 ± 0.03	3.39 ± 0.03	3.51 ± 0.03	3.61 ± 0.04			3.71 ± 0.04
pH	5.1 ± 0.1	4.5 ± 0.1	4.5 ± 0.1	4.8 ± 0.1	4.8 ± 0.1	4.8 ± 0.1	5.0 ± 0.1	5.3 ± 0.1			5.6 ± 0.1

**Table 2**  $\log_{10} F\beta_1$  (M) data ( $\text{NaNO}_3$  and  $\text{NaCl}$ ) at 25 °C {molal ( $\text{mol}\cdot\text{kg}^{-1}$ ) scale}

<i>I</i> ( $\text{mol}\cdot\text{kg}^{-1}$ )	$\log_{10} F\beta_1$ (M) in $\text{NaNO}_3$					$\log_{10} F\beta_1$ (M) in $\text{NaCl}$				
	0.7	1.5	3.0	4.0	5.0	0.7	1.5	3.0	4.0	5.0
St. dev.	$\pm 0.03$	$\pm 0.03$	$\pm 0.03$	$\pm 0.03$	$\pm 0.04$	$\pm 0.03$	$\pm 0.03$	$\pm 0.03$	$\pm 0.03$	$\pm 0.04$
Y	3.446	3.397	3.513	3.570	3.754	3.408	3.370	3.393	3.469	3.550
La	2.610	2.559	2.650	2.798	3.099	2.571	2.531	2.524	2.640	2.795
Ce	2.830	2.784	2.920	3.034	3.310	2.804	2.764	2.800	2.864	3.013
Pr	2.821	2.779	2.899	3.023	3.287	2.793	2.753	2.764	2.864	2.998
Nd	2.807	2.765	2.860	3.001	3.277	2.778	2.738	2.747	2.838	2.975
Pm										
Sm	3.140	3.080	3.158	3.246	3.432	3.113	3.066	3.057	3.160	3.219
Eu	3.257	3.199	3.270	3.357	3.554	3.222	3.189	3.188	3.274	3.348
Gd	3.208	3.150	3.243	3.301	3.487	3.178	3.150	3.152	3.222	3.258
Tb	3.339	3.277	3.365	3.434	3.621	3.320	3.271	3.291	3.384	3.446
Dy	3.372	3.314	3.412	3.468	3.654	3.333	3.290	3.303	3.415	3.480
Ho	3.260	3.245	3.281	3.346	3.532	3.234	3.201	3.200	3.302	3.361
Er	3.261	3.208	3.293	3.357	3.531	3.228	3.180	3.207	3.292	3.332
Tm	3.274	3.219	3.313	3.358	3.532	3.244	3.194	3.205	3.303	3.363
Yb	3.372	3.326	3.430	3.479	3.654	3.341	3.298	3.322	3.397	3.480
Lu	3.233	3.183	3.295	3.346	3.511	3.203	3.153	3.194	3.274	3.336
pH	$4.8 \pm 0.1$	$4.8 \pm 0.1$	$4.8 \pm 0.1$	$5.0 \pm 0.1$	$5.3 \pm 0.1$	$4.8 \pm 0.1$	$4.8 \pm 0.1$	$4.8 \pm 0.1$	$5.0 \pm 0.1$	$5.3 \pm 0.1$

**Table 3**  $\log_{10} F \beta_1^0(M)$ ,  $B$ , and  $C$  values calculated using Eq. 7 (NaClO<sub>4</sub>, NaNO<sub>3</sub>, NaCl)

M	$\log_{10} F \beta_1^0(M)$	B		C			
		NaClO <sub>4</sub>	NaNO <sub>3</sub>	NaClO <sub>4</sub>	NaCl	NaNO <sub>3</sub>	NaCl
Y	4.445 ± 0.03	1.815 ± 0.13	1.549 ± 0.06	1.578 ± 0.04	0.147 ± 0.01	0.165 ± 0.01	0.124 ± 0.01
La	3.653 ± 0.05	1.513 ± 0.19	1.276 ± 0.12	1.381 ± 0.07	0.205 ± 0.03	0.232 ± 0.02	0.159 ± 0.02
Ce	3.893 ± 0.04	1.484 ± 0.13	1.274 ± 0.08	1.415 ± 0.05	0.206 ± 0.03	0.231 ± 0.02	0.150 ± 0.01
Pr	3.869 ± 0.03	1.533 ± 0.13	1.313 ± 0.08	1.419 ± 0.05	0.194 ± 0.02	0.223 ± 0.02	0.151 ± 0.01
Nd	3.837 ± 0.04	1.593 ± 0.15	1.336 ± 0.10	1.465 ± 0.06	0.187 ± 0.02	0.221 ± 0.02	0.146 ± 0.01
Pm							
Sm	4.167 ± 0.03	1.716 ± 0.13	1.455 ± 0.06	1.533 ± 0.05	0.148 ± 0.01	0.170 ± 0.01	0.121 ± 0.01
Eu	4.279 ± 0.04	1.750 ± 0.17	1.464 ± 0.07	1.543 ± 0.05	0.145 ± 0.02	0.169 ± 0.01	0.123 ± 0.01
Gd	4.240 ± 0.04	1.753 ± 0.14	1.467 ± 0.06	1.581 ± 0.07	0.144 ± 0.01	0.165 ± 0.01	0.110 ± 0.01
Tb	4.383 ± 0.03	1.727 ± 0.12	1.428 ± 0.06	1.505 ± 0.04	0.148 ± 0.01	0.169 ± 0.01	0.129 ± 0.01
Dy	4.393 ± 0.03	1.747 ± 0.12	1.494 ± 0.06	1.500 ± 0.05	0.148 ± 0.01	0.163 ± 0.01	0.134 ± 0.01
Ho	4.268 ± 0.03	1.825 ± 0.14	1.584 ± 0.05	1.595 ± 0.05	0.143 ± 0.01	0.148 ± 0.02	0.120 ± 0.02
Er	4.262 ± 0.03	1.807 ± 0.11	1.555 ± 0.06	1.603 ± 0.05	0.145 ± 0.01	0.154 ± 0.01	0.117 ± 0.01
Tm	4.279 ± 0.03	1.822 ± 0.12	1.558 ± 0.06	1.572 ± 0.04	0.142 ± 0.01	0.152 ± 0.01	0.122 ± 0.01
Yb	4.378 ± 0.03	1.799 ± 0.11	1.556 ± 0.06	1.573 ± 0.03	0.147 ± 0.01	0.158 ± 0.01	0.124 ± 0.01
Lu	4.241 ± 0.03	1.778 ± 0.11	1.552 ± 0.05	1.585 ± 0.03	0.150 ± 0.01	0.158 ± 0.01	0.123 ± 0.01



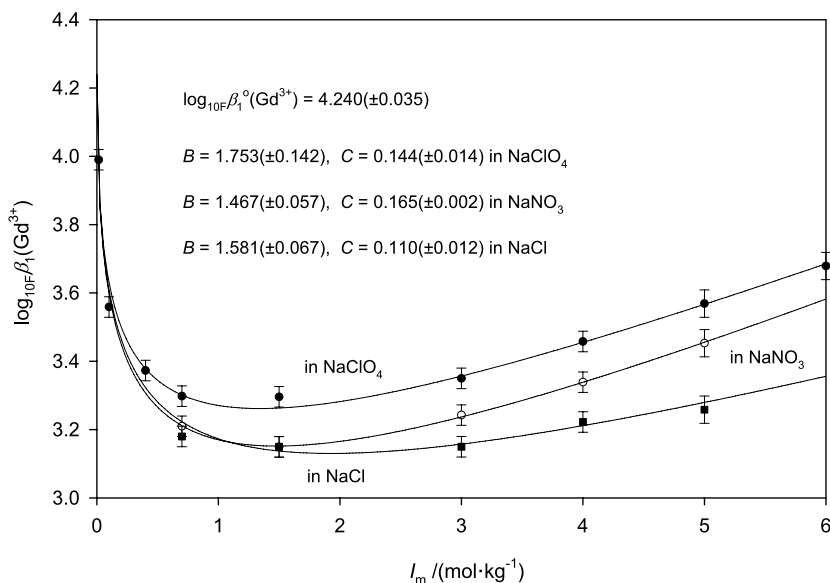


**Fig. 2** Dependence of  $\log_{10} F \beta_1(\text{Gd})$  on ionic strength in  $\text{NaClO}_4$ ,  $\text{NaNO}_3$  and  $\text{NaCl}$  solutions

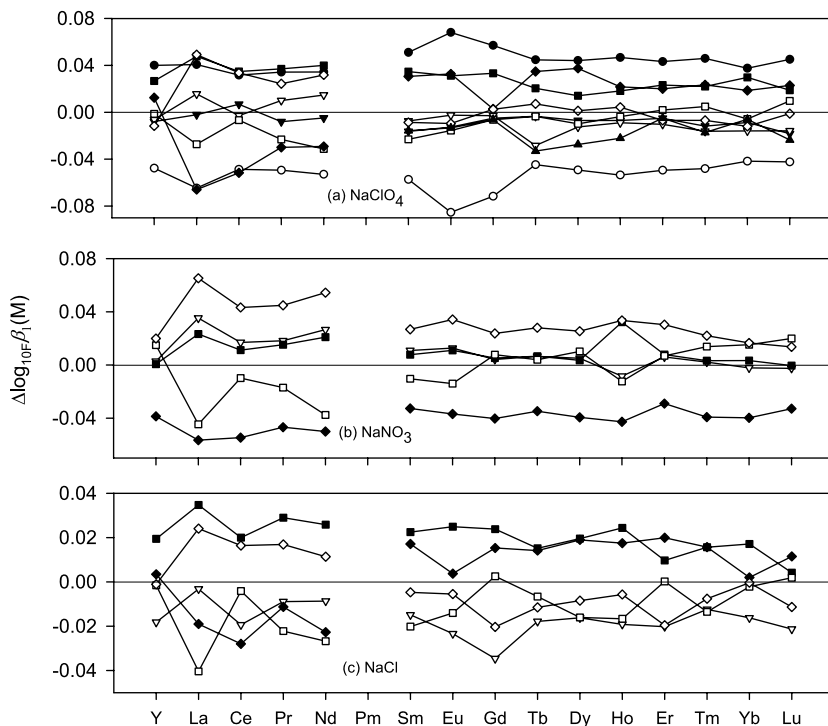


**Fig. 3** Residuals for Eq. 7  $\log_{10} F \beta_1(\text{M})$  regressions: **a**  $\text{NaClO}_4$ ; **b**  $\text{NaNO}_3$ ; **c**  $\text{NaCl}$ ; experimental conditions,  $I$  ( $\text{mol}\cdot\text{kg}^{-1}$ ): (●) 0.015, (○) 0.1, (▼) 0.4, (▽) 0.7, (■) 1.5, (□) 3.0, (◆) 4.0, (◇) 5.0, (▲) 6.0

**Table 4**  $\log_{10} F\beta_1^0(M)$  and  $C$  calculated using Eq. 8 ( $B = 1.5$ ) ( $\text{NaClO}_4$ ,  $\text{NaNNO}_3$ ,  $\text{NaCl}$ )

M	$\text{NaClO}_4$		$\text{NaNNO}_3$		$\text{NaCl}$	
	$\log_{10} F\beta_1^0$	$C$	$\log_{10} F\beta_1^0$	$C$	$\log_{10} F\beta_1^0$	$C$
Y	$4.507 \pm 0.05$	$0.184 \pm 0.01$	$4.466 \pm 0.03$	$0.168 \pm 0.01$	$4.473 \pm 0.02$	$0.132 \pm 0.05$
La	$3.656 \pm 0.05$	$0.206 \pm 0.01$	$3.567 \pm 0.06$	$0.206 \pm 0.02$	$3.605 \pm 0.03$	$0.146 \pm 0.01$
Ce	$3.890 \pm 0.05$	$0.204 \pm 0.01$	$3.799 \pm 0.05$	$0.206 \pm 0.02$	$3.857 \pm 0.02$	$0.142 \pm 0.01$
Pr	$3.876 \pm 0.05$	$0.198 \pm 0.01$	$3.795 \pm 0.05$	$0.203 \pm 0.01$	$3.836 \pm 0.02$	$0.144 \pm 0.01$
Nd	$3.856 \pm 0.05$	$0.200 \pm 0.01$	$3.776 \pm 0.05$	$0.202 \pm 0.02$	$3.823 \pm 0.02$	$0.141 \pm 0.01$
Pm						
Sm	$4.215 \pm 0.05$	$0.171 \pm 0.01$	$4.152 \pm 0.03$	$0.165 \pm 0.01$	$4.178 \pm 0.02$	$0.125 \pm 0.01$
Eu	$4.333 \pm 0.05$	$0.171 \pm 0.01$	$4.268 \pm 0.03$	$0.165 \pm 0.01$	$4.272 \pm 0.02$	$0.127 \pm 0.01$
Gd	$4.296 \pm 0.05$	$0.170 \pm 0.01$	$4.229 \pm 0.03$	$0.161 \pm 0.01$	$4.265 \pm 0.03$	$0.118 \pm 0.01$
Tb	$4.433 \pm 0.05$	$0.172 \pm 0.01$	$4.355 \pm 0.03$	$0.162 \pm 0.01$	$4.382 \pm 0.02$	$0.130 \pm 0.01$
Dy	$4.447 \pm 0.05$	$0.174 \pm 0.01$	$4.393 \pm 0.03$	$0.162 \pm 0.01$	$4.390 \pm 0.02$	$0.135 \pm 0.01$
Ho	$4.347 \pm 0.05$	$0.175 \pm 0.01$	$4.303 \pm 0.03$	$0.155 \pm 0.02$	$4.303 \pm 0.03$	$0.129 \pm 0.02$
Er	$4.329 \pm 0.05$	$0.177 \pm 0.01$	$4.286 \pm 0.02$	$0.159 \pm 0.01$	$4.298 \pm 0.02$	$0.126 \pm 0.01$
Tm	$4.349 \pm 0.05$	$0.174 \pm 0.01$	$4.304 \pm 0.02$	$0.157 \pm 0.01$	$4.306 \pm 0.02$	$0.128 \pm 0.01$
Yb	$4.442 \pm 0.05$	$0.177 \pm 0.01$	$4.401 \pm 0.03$	$0.162 \pm 0.01$	$4.404 \pm 0.03$	$0.131 \pm 0.01$
Lu	$4.302 \pm 0.05$	$0.179 \pm 0.01$	$4.262 \pm 0.02$	$0.162 \pm 0.01$	$4.272 \pm 0.01$	$0.131 \pm 0.01$

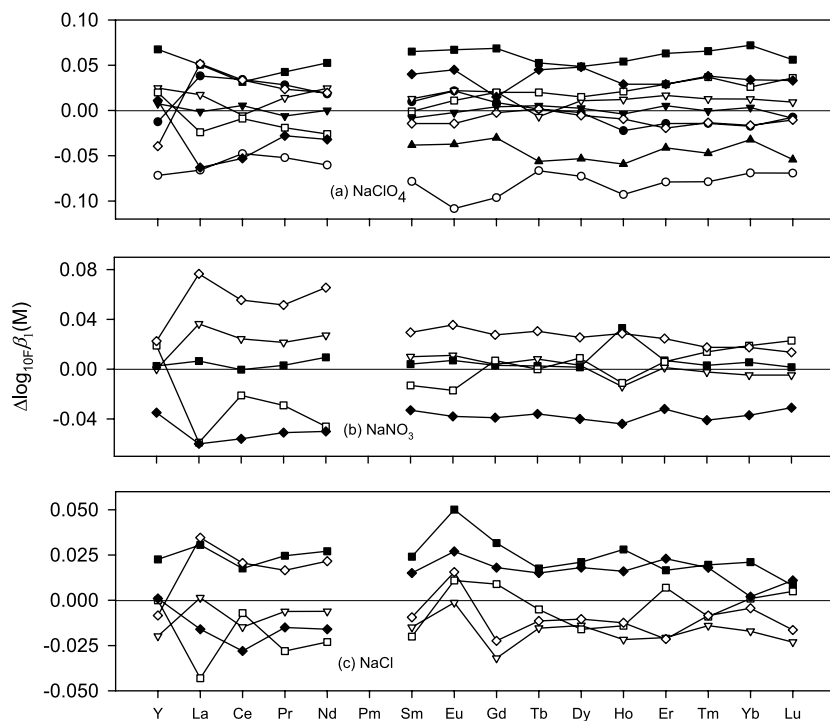


**Fig. 4** Residuals for Eq. 8  $\log_{10} F\beta_1(M)$  regressions: ( $B = 1.5$ ): **a**  $\text{NaClO}_4$ ; **b**  $\text{NaNO}_3$ ; **c**  $\text{NaCl}$ ; experimental conditions,  $I$  ( $\text{mol}\cdot\text{kg}^{-1}$ ): (●) 0.015, (○) 0.1, (▼) 0.4, (▽) 0.7, (■) 1.5, (□) 3.0, (◆) 4.0, (◇) 5.0, (▲) 6.0

uncertainties obtained in  $\text{NaCl}$  medium (Table 4) are all on the order of 0.025. The comparatively well defined  $\log_{10} F\beta_1^{\circ}(M)$  estimates obtained for perchlorate using Eq. 7 are compared in Fig. 5a with the Table 4  $\log_{10} F\beta_1^{\circ}(M)$  estimates obtained for  $\text{NaNO}_3$  and  $\text{NaCl}$  using Eq. 8. With the exception of the data obtained for light YREEs in  $\text{NaNO}_3$  that have uncertainties on the order of 0.05, all of the patterns shown in Fig. 5a are quite consistent.

The shape of  $\log_{10} F\beta_1(M)$  patterns is only weakly dependent on ionic strength and medium composition. Figure 5b provides a comparison of  $\log_{10} F\beta_1(M)$  patterns in  $\text{NaClO}_4$ ,  $\text{NaNO}_3$  and  $\text{NaCl}$  at  $4.0 \text{ mol}\cdot\text{kg}^{-1}$  ionic strength. Comparisons of Figs. 5a and 5b demonstrate that differences in the shapes of  $\log_{10} F\beta_1(M)$  patterns due to changes in ionic strength and medium composition are subtle. Insight into the influence of ionic strength on  $\log_{10} F\beta_1(M)$  patterns can be gained by examination of the ‘ $B$ ’ and ‘ $C$ ’ parameters in Table 3. Although the ‘ $B$ ’ and ‘ $C$ ’ values in Table 3 vary somewhat between the lightest REEs (La, Ce, Pr, Nd) and the heavy YREEs (Sm through Lu), the ‘ $B$ ’ and ‘ $C$ ’ parameters shown for the heavy YREEs in a given medium are highly consistent. The ‘ $B$ ’ and ‘ $C$ ’ parameters obtained in  $\text{NaClO}_4$  for the YREEs between Sm and Lu can be summarized as  $B = 1.772 \pm 0.039$  and  $C = 0.146 \pm 0.003$ . For the lightest REEs (La, Ce, Pr, Nd), the average ‘ $B$ ’ and ‘ $C$ ’ parameters in  $\text{NaClO}_4$  are  $B = 1.531 \pm 0.046$  and  $C = 0.198 \pm 0.009$ . Similar behavior for ‘ $B$ ’ and ‘ $C$ ’ parameters were obtained in  $\text{NaNO}_3$  and  $\text{NaCl}$  solutions: yttrium and the elements from Sm to Lu have very similar ‘ $B$ ’ and ‘ $C$ ’ parameters, and the corresponding parameters for La through Nd differ somewhat from the parameters for Y and the heavy REEs. Based on these observations it is expected that  $\text{MF}^{2+}$  stability constant

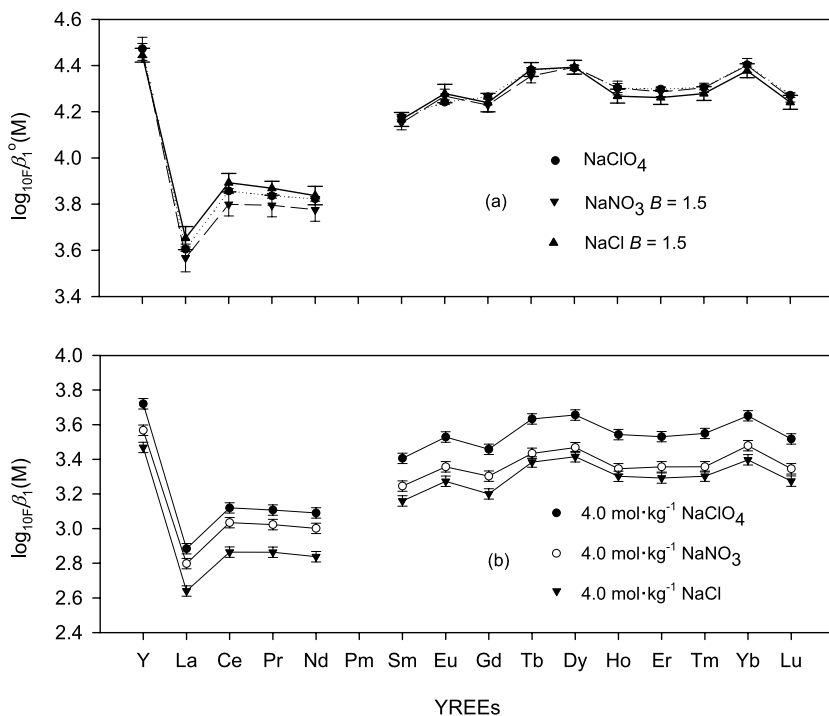


**Fig. 5** **a** Comparison of  $\log_{10} F\beta_1^\circ(M)$  obtained in  $\text{NaClO}_4$ ,  $\text{NaNO}_3$  and  $\text{NaCl}$  solutions. **b** Comparison of  $\log_{10} F\beta_1(M)$  in  $4.0 \text{ mol}\cdot\text{kg}^{-1}$   $\text{NaClO}_4$ ,  $\text{NaNO}_3$  and  $\text{NaCl}$  solutions

patterns will exhibit only subtle changes with ionic strength for Y and Sm through Lu, and formation constant changes with ionic strength for La through Nd will be somewhat distinct from the behavior of Y and the heavier REEs.

In addition to descriptions of the influence of medium composition on  $\log_{10} F\beta_1(M)$  in terms of Debye–Hückel parameters and specific interaction parameters (i.e., ‘*B*’ and ‘*C*’ parameters), differences in  $\log_{10} F\beta_1(M)$  obtained in  $\text{NaClO}_4$ ,  $\text{NaNO}_3$  and  $\text{NaCl}$  can be described in terms of YREE complexation by nitrate and chloride ions. Table 5 provides a compilation of  $\log_{10} \text{NO}_3\beta_1(M)$  and  $\log_{10} \text{Cl}\beta_1(M)$  results calculated using Eqs. 5 and 6 and the  $\log_{10} F\beta_1(M)$  data shown in Tables 1 and 2. Due to the small differences between  $\log_{10} F\beta_1(M)$  results obtained in  $\text{NaClO}_4$  and  $\text{NaNO}_3$  (e.g., Figs. 2 and 5b),  $\log_{10} \text{NO}_3\beta_1(M)$  results are somewhat less well defined than the results obtained for  $\log_{10} \text{Cl}\beta_1(M)$ . Inspection of the  $\log_{10} \text{NO}_3\beta_1(M)$  data in Table 5 between  $0.7$  and  $3.0 \text{ mol}\cdot\text{kg}^{-1}$  ionic strength shows little evidence of significant trends across the suite of YREEs. At  $0.7 \text{ mol}\cdot\text{kg}^{-1}$  ionic strength, for example, the average  $\log_{10} \text{NO}_3\beta_1(M)$  result for all elements is  $-0.59 \pm 0.05$ , and at  $3.0 \text{ mol}\cdot\text{kg}^{-1}$  ionic strength the average  $\log_{10} \text{NO}_3\beta_1(M)$  result for all elements is  $-1.04 \pm 0.08$ . Results shown in Table 5, however, are suggestive of significant distinctions between light and heavy element complexation by  $\text{NO}_3^-$  at higher ionic strengths. In contrast, results obtained for  $\log_{10} \text{Cl}\beta_1(M)$ , which are better defined than the  $\log_{10} \text{NO}_3\beta_1(M)$  results, show little evidence of differences in the behavior of lighter and heavier elements. As a first-order description of the  $\log_{10} \text{NO}_3\beta_1(M)$  and  $\log_{10} \text{Cl}\beta_1(M)$  results shown in Table 5, Fig. 6 shows a depiction of stability constant results wherein it is assumed that the formation

**Table 5**  $\log_{10} \text{NO}_3\beta_1$  (M) and  $\log_{10} \text{Cl}\beta_1$  (M) at 25 °C (molar ( $\text{mol}\cdot\text{kg}^{-1}$ ) scale)

I ( $\text{mol}\cdot\text{kg}^{-1}$ )	$\log_{10} \text{NO}_3\beta_1$ (M)					$\log_{10} \text{Cl}\beta_1$ (M)				
	0.7	1.5	3.0	4.0	5.0	0.7	1.5	3.0	4.0	5.0
Y	-0.557	-0.633	-1.115	-0.983	-1.536	-0.363	-0.537	-0.683	-0.706	-0.779
La	-0.602	-0.622	-0.958	-1.262	-1.498	-0.390	-0.524	-0.586	-0.725	-0.574
Ce	-0.674	-0.673	-1.079	-1.262	-1.536	-0.505	-0.596	-0.665	-0.697	-0.595
Pr	-0.602	-0.703	-1.196	-1.273	-1.876	-0.442	-0.600	-0.681	-0.727	-0.668
Nd	-0.564	-0.673	-1.094	-1.240	-1.944	-0.408	-0.571	-0.691	-0.704	-0.650
Pm										
Sm	-0.602	-0.622	-1.099	-0.953	-1.622	-0.447	-0.571	-0.726	-0.720	-0.781
Eu	-0.539	-0.618	-1.013	-0.915	-1.661	-0.363	-0.582	-0.729	-0.700	-0.806
Gd	-0.483	-0.574	-1.031	-0.963	-1.381	-0.342	-0.574	-0.715	-0.744	-0.679
Tb	-0.570	-0.585	-0.942	-0.838	-1.291	-0.488	-0.564	-0.705	-0.713	-0.755
Dy	-0.602	-0.677	-1.084	-0.868	-1.376	-0.390	-0.585	-0.697	-0.732	-0.792
Ho	-0.516	-0.673	-0.912	-0.843	-1.257	-0.385	-0.600	-0.665	-0.732	-0.748
Er	-0.596	-0.649	-0.974	-0.903	-1.342	-0.413	-0.547	-0.694	-0.732	-0.725
Tm	-0.589	-0.622	-0.979	-0.857	-1.291	-0.422	-0.534	-0.640	-0.718	-0.768
Yb	-0.609	-0.633	-1.099	-0.915	-1.381	-0.432	-0.534	-0.707	-0.702	-0.794
Lu	-0.652	-0.673	-1.045	-0.915	-1.281	-0.467	-0.561	-0.697	-0.725	-0.751
Average	-0.586	-0.642	-1.041	-0.999	-1.485	-0.417	-0.565	-0.686	-0.718	-0.724
St. dev.	0.05	0.04	0.08	0.17	0.21	0.05	0.03	0.04	0.02	0.07

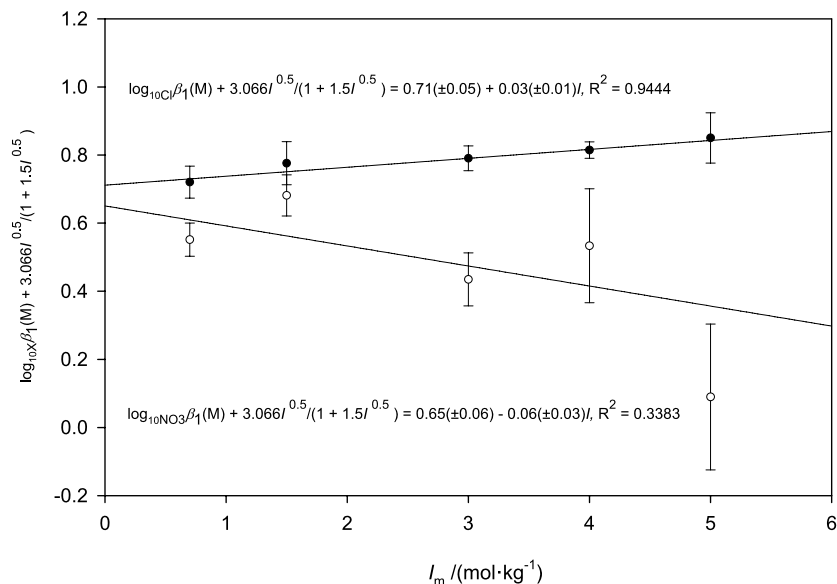


**Fig. 6** Dependence of  $\log_{10} \text{NO}_3 \beta_1 (\text{M})$  and  $\log_{10} \text{Cl} \beta_1 (\text{M})$  on ionic strength

constants of  $\text{MNO}_3^{2+}$  and  $\text{MCl}^{2+}$  are invariant, at constant ionic strength, across the entire suite of YREEs. Figure 6 shows that YREE nitrate stability constants can be summarized as

$$\log_{10} \text{NO}_3 \beta_1 (\text{M}^{3+}) + \frac{3.066 I^{0.5}}{1 + 1.5 I^{0.5}} = 0.65 (\pm 0.06) - 0.06 (\pm 0.03) I, \quad R^2 = 0.3383 \quad (9)$$

and YREE chloride stability constants are given as

$$\log_{10} \text{Cl} \beta_1 (\text{M}^{3+}) + \frac{3.066 I^{0.5}}{1 + 1.5 I^{0.5}} = 0.71 (\pm 0.05) + 0.03 (\pm 0.01) I, \quad R^2 = 0.9444. \quad (10)$$

Using Eqs. 9 and 10, and the stability constants given in Table 5, Figs. 7a and 7b show residuals in the form  $\Delta \log_{10} \text{NO}_3 \beta_1 (\text{M}) = (\log_{10} \text{NO}_3 \beta_1 (\text{observed}) - \log_{10} \text{NO}_3 \beta_1 (\text{predicted}))$  and  $\Delta \log_{10} \text{Cl} \beta_1 (\text{M}) = (\log_{10} \text{Cl} \beta_1 (\text{observed}) - \log_{10} \text{Cl} \beta_1 (\text{predicted}))$ . The Fig. 7a residual plot for  $\log_{10} \text{NO}_3 \beta_1 (\text{M})$  predictions shows that  $\text{MNO}_3^{2+}$  stability constants (Table 5) can be predicted within approximately 0.2 log units using Eq. 9 between ionic strengths of 0.7 and 4.0  $\text{mol} \cdot \text{kg}^{-1}$ . All of the  $\log_{10} \text{NO}_3 \beta_1 (\text{M})$  data in Table 5, with the exception of the data for Pr, Nd, Sm and Eu at 5.0  $\text{mol} \cdot \text{kg}^{-1}$  ionic strength, can be predicted within  $\pm 0.3$  log units using Eq. 9. Figure 7b shows that Eq. 10 can be used to predict nearly all the Table 5  $\log_{10} \text{Cl} \beta_1 (\text{M})$  data within 0.1 log units. With the exception of the  $\text{MCl}^{2+}$  stability constants obtained at 5.0  $\text{mol} \cdot \text{kg}^{-1}$  ionic strength, Eq. 10 predicts most of the Table 5  $\log_{10} \text{Cl} \beta_1 (\text{M})$  values within approximately 0.05 log units.

The  $\log_{10} \text{Cl} \beta_1^0 (\text{M})$  result obtained in this work ( $\log_{10} \text{Cl} \beta_1^0 (\text{M}) = 0.71 \pm 0.05$ ) is in good agreement with the result ( $\log_{10} \text{Cl} \beta_1^0 (\text{M}) = 0.65 \pm 0.05$ ) of Luo and Byrne [18]. Both of these results are in fair agreement with the results of Mironov et al. [20] wherein  $\log_{10} \text{Cl} \beta_1^0 (\text{M})$  results ranged from 0.48 for  $\log_{10} \text{Cl} \beta_1^0 (\text{La})$  to 0.23 for  $\log_{10} \text{Cl} \beta_1^0 (\text{Lu})$ . Our results contrast with those of Mironov et al. [20], however, in that  $\log_{10} \text{Cl} \beta_1 (\text{M})$  results ob-

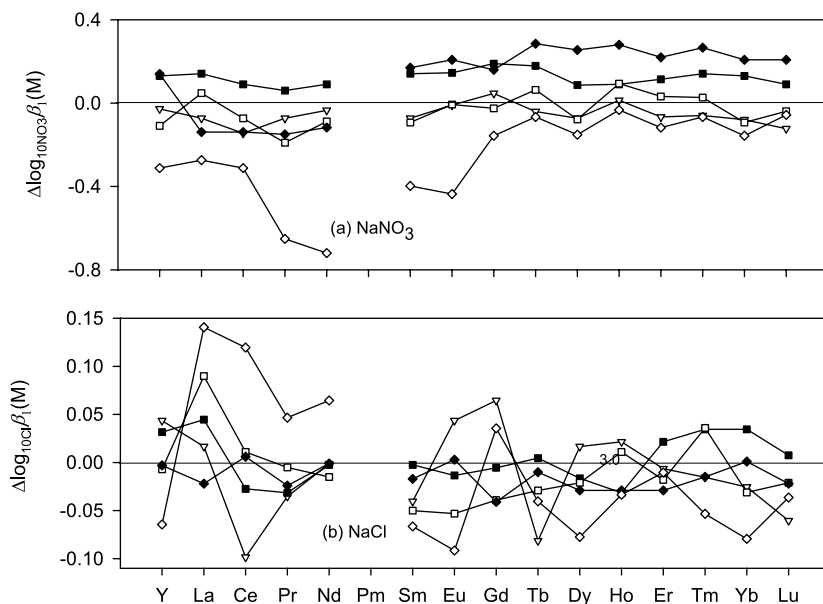


**Fig. 7** Residuals for Eq. 9  $\log_{10} \text{NO}_3 \beta_1 (\text{M})$  regressions and Eq. 10  $\log_{10} \text{Cl} \beta_1 (\text{M})$  regressions; experimental conditions,  $I$  ( $\text{mol} \cdot \text{kg}^{-1}$ ); ( $\nabla$ ) 0.7, ( $\blacksquare$ ) 1.5, ( $\square$ ) 3.0, ( $\blacklozenge$ ) 4.0, ( $\diamond$ ) 5.0

tained in the present study are constant, at a given ionic strength, across the entire suite of YREEs.

## 5 Conclusions

Stability constants of YREE fluoride complexes ( $\text{MF}^{2+}$ ), determined in  $\text{NaClO}_4$ ,  $\text{NaNO}_3$  and  $\text{NaCl}$  over a wide range of ionic strength, show highly consistent patterns across the fifteen-member suite of YREEs. The ability of an analytical procedure to reproduce the stability constant pattern observed in this work, and a limited number of previous works, can serve as a useful indicator of the procedure's analytical quality. Such an assessment is only available when YREE stability constants are determined as a suite rather than one or only a few elements. Determination of YREE stability constants as a suite is also important as a means of enabling precise assessments of the influence of solution complexation on environmental patterns of YREE fractionation.

The magnitudes of  $\log_{10} \text{F} \beta_1 (\text{M})$  are dependent on medium composition. Our work shows that  $\log_{10} \text{F} \beta_1 (\text{M})$  results obtained in  $\text{NaClO}_4$  are consistently larger than  $\log_{10} \text{F} \beta_1 (\text{M})$  results obtained in  $\text{NaNO}_3$  which, in turn, are larger than  $\log_{10} \text{F} \beta_1 (\text{M})$  results obtained in chloride solutions. The medium dependence of YREE-fluoride complexation can be quantitatively explained in terms of YREE complexation by nitrate and chloride ions. Both nitrate ions and chloride ions complex YREEs weakly, and the stability constant patterns of  $\log_{10} \text{NO}_3 \beta_1 (\text{M})$  and  $\log_{10} \text{Cl} \beta_1 (\text{M})$  across the entire suite of YREEs appear to be essentially flat. At zero ionic strength and  $25^\circ \text{C}$ ,  $\log_{10} \text{NO}_3 \beta_1^0 (\text{M}) = 0.65 \pm 0.06$  and  $\log_{10} \text{Cl} \beta_1^0 (\text{M}) = 0.71 \pm 0.05$ .

**Acknowledgements** This work was supported by a grant from the National Science Foundation (OCE-0136333).

## Appendix

Metal	$[M^{3+}]_{IT}$ $\times 10^4/\text{mol}\cdot\text{L}^{-1}$	Medium: $\text{NaNO}_3$ $[\text{F}^-] \times 10^5/\text{mol}\cdot\text{L}^{-1}$				Medium: $\text{NaCl}$ $[\text{F}^-] \times 10^5/\text{mol}\cdot\text{L}^{-1}$					
		0.7m	1.5m	3.0m	4.0m	5.0m	0.7m	1.5m	3.0m	4.0m	5.0m
Y	9.90	2.81	3.30	2.02	1.50	0.802	2.83	3.50	2.90	2.40	1.40
La	9.89	7.31	7.82	6.93	6.50	4.80	8.30	8.78	8.85	7.50	5.50
Ce	9.89	6.05	6.28	5.51	4.62	3.35	6.15	6.44	6.30	5.88	4.76
Pr	9.90	6.11	6.33	5.70	4.87	3.65	6.18	6.33	6.25	5.90	4.85
Nd	9.91	6.40	6.61	5.80	5.09	3.80	6.48	6.65	6.56	6.25	5.00
Pm											
Sm	9.91	4.82	5.10	4.56	3.80	3.00	5.00	5.59	5.66	4.50	3.75
Eu	9.90	3.84	4.11	3.45	2.70	1.75	4.01	4.30	4.40	3.20	2.70
Gd	9.91	4.09	4.35	3.80	3.00	2.24	4.12	4.80	4.82	3.32	2.85
Tb	9.87	3.70	3.90	3.45	2.80	2.02	4.04	4.50	4.40	3.15	2.45
Dy	9.89	3.51	3.68	3.25	2.66	1.68	3.78	4.20	4.10	2.95	2.30
Ho	9.92	3.77	4.02	3.60	3.03	2.13	3.99	4.31	4.28	3.25	2.71
Er	9.89	3.79	4.05	3.59	2.98	2.10	3.98	4.32	4.10	3.22	2.72
Tm	9.88	3.71	3.90	3.50	2.93	2.06	4.01	4.30	4.25	3.20	2.70
Yb	9.92	3.21	3.51	3.00	2.40	1.50	3.70	4.10	3.80	3.00	2.20
Lu	9.92	3.90	4.15	3.70	3.14	2.32	4.10	4.40	4.20	3.50	3.00
pH		4.8 ± 0.1	4.8 ± 0.1	4.8 ± 0.1	5.0 ± 0.1	5.3 ± 0.1	4.8 ± 0.1	4.8 ± 0.1	4.8 ± 0.1	5.0 ± 0.1	5.3 ± 0.1
<i>f</i>		1.0225	1.0488	1.1072	1.1509	1.1964	1.0158	1.0324	1.0683	1.0963	1.1284

$[\text{F}^-]_{IT} = 9.80 \times 10^{-5} \text{ mol}\cdot\text{L}^{-1}$  for all experiments, and  $(\text{mol}\cdot\text{L}^{-1}) \times f = \text{mol} \cdot (\text{kg}\cdot\text{H}_2\text{O})^{-1}$



## References

1. Byrne, R.H., Sholkovitz, E.R.: In: Gschneidner Jr., K.A., Eyring, L. (eds.) Handbook on the Physics and Chemistry of Rare Earths, vol. 23. Elsevier, Amsterdam (1996), Chap. 158
2. Quinn, K.A., Byrne, R.H., Schijf, J.: Sorption of yttrium and rare earth elements by amorphous ferric hydroxide: Influence of pH and ionic strength. *Marine Chem.* **99**, 128–150 (2006)
3. Byrne, R.H., Kim, K.H.: Rare earth element scavenging in seawater. *Geochim. Cosmochim. Acta* **54**, 2645–2656 (1990)
4. Lee, J.H., Byrne, R.H.: Complexation of trivalent rare earth elements (cerium, europium, gadolinium, terbium, and ytterbium) by carbonate ions. *Geochim. Cosmochim. Acta* **57**, 295–302 (1993)
5. Luo, Y.R., Byrne, R.H.: The ionic strength dependence of rare earth and yttrium fluoride complexation at 25 °C. *J. Solution Chem.* **29**, 1089–1099 (2000)
6. Luo, Y., Millero, F.J.: Effects of temperature and ionic strength on the stabilities of the first and second fluoride complexes of yttrium and the rare earth elements. *Geochim. Cosmochim. Acta* **68**, 4301–4308 (2004)
7. Schijf, J., Byrne, R.H.: Determination of stability constants for the mono- and difluoro-complexes of Y and the REE, using a cation-exchange resin and ICP-MS. *Polyhedron* **18**, 2839–2844 (1999)
8. Lee, J.H., Byrne, R.H.: Rare earth element complexation by fluoride ions in aqueous solution. *J. Solution Chem.* **22**, 751–766 (1993)
9. Walker, J.B., Choppin, G.R.: Thermodynamic parameters of fluoride complexes of the lanthanides. *Adv. Chem. Ser.* **71**, 127–140 (1967)
10. Avramenko, N.I., Andronov, E.A., Blokhin, V.V., Mironov, V.E.: Study of fluoride complexes of rare earth metals in aqueous salt solutions. *Izv. Vyssh. Uchebn. Zaved. Khim. Tekhnol.* **26**, 155–157 (1983) (in Russian)
11. Bilal, B.A., Herrmann, F., Fleischer, W.: Complex formation of trace elements in geochemical systems. 1. Potentiometric study of fluoro complexes of rare earth elements in fluorite bearing model systems. *J. Inorg. Nucl. Chem.* **41**, 347–350 (1979)
12. Bilal, B.A., Becker, P.: Complex formation of trace elements in geochemical systems. 2. Stability of rare earths fluoro complexes in fluorite bearing model system at various ionic strengths. *J. Inorg. Nucl. Chem.* **41**, 1607–1608 (1979)
13. Bilal, B.A., Kob, V.: Complex formation of trace elements in geochemical systems. 3. Studies on the distribution of fluoro complexes of rare earth elements in fluorite bearing model systems. *J. Inorg. Nucl. Chem.* **42**, 629–630 (1980)
14. Bilal, B.A., Koss, V.: Complex formation of trace elements in geochemical systems. 4. Study on the distribution of sulfatocomplexes of rare earth elements in fluorite-bearing model system. *J. Inorg. Nucl. Chem.* **42**, 1064–1065 (1980)
15. Becker, P., Bilal, B.P.: Lanthanide–fluoride ion association in aqueous sodium chloride solutions at 25 °C. *J. Solution Chem.* **14**, 407–415 (1985)
16. Menon, M.P., James, J., Jackson, J.D.: Studies on the solubility and complexation of lanthanum and neodymium fluoride–water systems. *Lanthan. Actinide Res.* **2**, 49–66 (1987)
17. Menon, M.P., James, J.: Solubilities, solubility products and solution chemistry of lanthanon trifluoride–water systems. *J. Chem. Soc. Faraday Trans. 1* **85**, 2683–2694 (1989)
18. Luo, Y.R., Byrne, R.H.: Yttrium and rare earth element complexation by chloride ions at 25 °C. *J. Solution Chem.* **30**, 837–845 (2001)
19. Smith, S.M., Martell, A.E.: NIST critically selected stability constants of metal complexes database, Version **8.0** (2004)
20. Mironov, V.E., Avramenko, N.I., Kopyrin, A.A., Blokhin, V.V., Eike, M.Yu., Isaev, I.D.: Thermodynamics of the formation of monochloride complexes of rare earth metals in aqueous solutions. *Koord. Khim.* **8**, 636–638 (1982) (in Russian)